On the existence and consistent approximation of long time classical trajectories and applications for molecular systems

Johannes Zimmer

Work with Hartmut Schwetlick (Bath)

Calculation of classical trajectories

The mathematical problem

Given the conservative dynamical system

$$\frac{d^2 q(t)}{\mathrm{d}t^2} = -\nabla V(q), \tag{1}$$

where V is a smooth potential on $Q \subset \mathbb{R}^n$, study the existence and consistent approximation of the *boundary value problem*:

$$q(0) = q_a \text{ and } q(T) = q_b \tag{2}$$

with $q_a, q_b \in Q$ and $T > 0$. Here, T is to be determined. Here V is the potential energy, E the total energy and $Q := \{q \mid V(q) < E\}$.

Motivation

Given a potential energy surface and two points (e.g., minima) in this landscape, find the Hamiltonian trajectory that connects the two — or, in practice, find a good approximation to the dynamical path.

Background

Motivation

- Complex systems in physics, chemistry or biology often have a potential energy landscape with many wells, separated by barriers
- Example: thermally activated reactions. Reactants will spend most of the time jostling around in one well before a rare spontaneous fluctuation occurs that lifts the atoms of the reactant over the barrier into the next (product) valley
- Such rare events easily exceed modern computing power (for example, configurational changes in DNA: dimension $n \approx 200$).

Relevant literature

- The system with periodic boundary conditions is well studied (e.g., Seifert, *Math. Z.*, **51** (1948), 197–216; Rabinowitz, *Comm. Pure Appl. Math.*, **31** (1978), 157–184).
- Boundary value problem much less studied (Gordon, *J. Differential Geometry*, **9** (1974), 443–450; related Benci, Fortunato, Giannoni, *Ann. Scuola Norm. Sup. Pisa Cl. Sci. (4)*, **19** (1992), 255–289)

Motivation

Molecular Dynamics (MD) simulation

Computation of molecular trajectories, e.g., with the Verlet algorithm.
Open:

- is the computed trajectory near a real one (shadowing);
- if so, is it near a generic trajectory.

Shadowing: mathematical results relying on hyperbolicity not applicable (Gillilan and Wilson, *J. Chem. Phys.*, **97** (1992), 1757–1772).

> *Hence, our trust in Molecular Dynamics simulation as a tool to study the time evolution of many-body systems is based largely on belief. To conclude this discussion, let us say that there is clearly still a corpse in the closet. We believe this corpse will not haunt us, and we quickly close the closet.*
>
> Frenkel & Smit, "Understanding Molecular Simulation", CUP

$\Longrightarrow$ develop convergent method, albeit not necessarily efficient.

Continuous setting

Hamilton's principle

Every dynamic trajectory with $q(0) = q_a$ and $q(T) = q_b$ is stationary point (saddle point; minimum only for nearby q_a, q_b) of the *action*

$$S[\gamma] := \int_0^T L\left(\gamma(t), \dot{\gamma}(t)\right) \mathrm{d}t \qquad \text{with } L(q, \dot{q}, \tau) = \frac{\langle \dot{q}, \dot{q} \rangle}{2} - V(q) \ . \quad (3)$$

Passerone and Parrinello, *Phys. Rev. Lett.*, **87** (2001), 108302
Passerone, Ceccarelli and Parrinello, *J. Chem. Phys.*, **118** (2003), 2025–2032: Augmentation of Hamilton's principle via the addition of constraints to transform it into a minimum principle.

Equivalent variational principle: Maupertuis / Jacobi

For $q = q(s)$ with $q(0) = q_a$ and $q(\tau) = q_b$, the *Maupertuis action* is

$$L[\gamma] := \int_0^\tau \sqrt{2(E - V(q))}\sqrt{\langle \dot{q}, \dot{q} \rangle}\, \mathrm{d}s = \int_0^\tau \sqrt{g(q)\,(q', q')}\, \mathrm{d}s \ . \quad (4)$$

Classic result: Hamiltonian trajectory is stationary point of S_M. We call this the *Jacobi's method* or *principle of stationary action*.

Birkhoff's algorithm

Summary so far

Hamiltonian boundary value problem is reformulated as variational problem (*elliptic* since *Jacobi metric* $g(q) := 2(E - V(q))\delta_{ij}$ is Riemann metric on Q). Solutions are *geodesics*, time can be recovered via formula $t = \int_0^\tau \sqrt{\frac{\langle q', q' \rangle}{2(E-V)}}\, \mathrm{d}s$.

Computation of geodesics in the continuous case

- Approximation converges to geodesic (possibly slowly)
- No refinement: number of chosen points remains constant.
- Problem: local geodesics nontrivial to compute in any metric other than the Euclidean metric (e.g., in Jacobi's metric!)

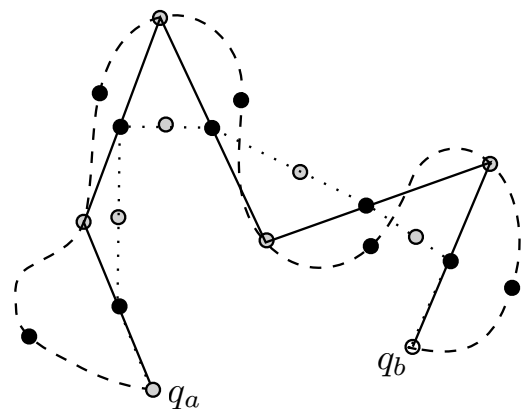

Figure: Birkhoff's algorithm (Euclidean metric in $\mathbb{R}^2$)

Computation of trajectories based on Jacobi's principle

Two different strategies

1. *Flow model:* Use that Hamiltonian equations can be equivalently reformulated as elliptic equation, and use parabolic flow ideas.
   - \+ Efficient computation
   - – At least hard to obtain convergence results
2. *Birkhoff approach:* use that trajectories are *geodesics*, use curve shortening.
   - \+ Convergence can be proved
   - – Algorithm more expensive than flow model

Other string methods

Gillilan and Wilson, *J. Chem. Phys.*, **97** (1992), 1757–1772 (Verlet action); Olender and Elber, *J. Chem. Phys.*, **105** (1996), 9299–9315 (Onsager-Machlup); Passerone, Ceccarelli and Parrinello, *J. Chem. Phys.*, **118** (2003), 2025–2032 (Hybrid Hamilton-Maupertuis iteration scheme); Banerjee and Adams, *J. Chem. Phys.*, **92** (1990), 7330–7339 (essentially Jacobi principle; linear combination of basis functions)

Outline of our approach

Elements of the argument

1. Use equivalent reformulation of the Hamiltonian system via Jacobi's principle (as Seifert, Weinstein, Gordon, ...).
   - Advantage: Hamiltonian system (normally unbounded from above and below) becomes elliptic (and thus bounded from below).
2. Then trajectories become geodesics. Use parabolic estimates to obtain invariant region for an associated flow with geodesic as limit.
3. Use discretisation of Jacobi metric and Birkhoff's method to develop constructive approach.

Step 1 is the same as in the case of periodic boundary conditions, Step 2 and 3 are new. Aim: bounds in terms of E and V rather than proper g-convexity (Gordon, *J. Differential Geometry*, **9** (1974), 443–450)

Caveat

No attempt is made to make the algorithm efficient; the aim is to give useful *a priori* bounds and prove existence. Algorithms inspired by this approach can be much faster (e.g., flow models).
Other method used: multiple shooting (for DNA in $\approx \mathbb{R}^{200}$).

Discrete Birkhoff method: fixed grid

Setting

Configuration: Given *Birkhoff triplet* (q_-, q, q_+) of the polygon,

$$q = (X, Y), q_\pm = (X_\pm, Y_\pm) \text{ with}$$

$$X_\pm = X \pm \epsilon, \in \mathbb{R}\ Y_\pm = Y + \Delta_\pm \in \mathbb{R}^{n-1},$$

we want to move q_0 in normal direction ν by length δ. Note: *two scales* ϵ and δ!

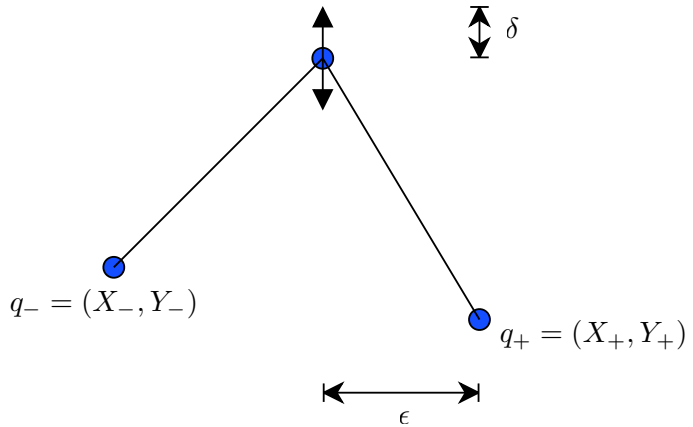

Define piecewise constant (=Euclidean) metric on grid of size ϵ, defining length $\bar{L}$.
Introduce piecewise constant approximation $\bar{g}$ of Jacobi metric g; this defines discrete length $\bar{L}$. Then consider *centred differences*

$$\Delta\bar{L}(\epsilon, \delta) := \left(\bar{L}(q_-, q + (0, \delta)) + \bar{L}(q + (0, \delta), q_+)\right) - \left(\bar{L}(q_-, q) + \bar{L}(q, q_+)\right).$$

This is the core quantity for the Jacobi algorithm.

Discrete Birkhoff method: fixed grid

Proposition

There exists $N > 0$ and $\epsilon_0 = \epsilon_0(N) > 0$ s.th. for all $\epsilon \in (0, \epsilon_0)$ and all triplets

$$q = (X, Y), q_\pm = (X_\pm, Y_\pm) \text{ with } X_\pm = X \pm \epsilon, \;\; Y_\pm = Y + \Delta_\pm$$

which satisfy $\left|\frac{\Delta_\pm}{\pm\epsilon}\right| \leq 1$ and $\frac{\Delta_+ + \Delta_-}{\epsilon^2} = -\hat{N}\hat{\nu}$, with $\hat{N} \in (N, 3N)$ and $\hat{\nu} \in S_\infty^{n-1}$, see figure, there holds

$$\begin{cases} \Delta\bar{L}(\epsilon, \delta) > 0 & \text{for every } \delta \text{ with } |\delta| \leq \epsilon^{\alpha+2} \text{ and } \frac{\delta}{|\delta|} \cdot \nu = 1, \\ \Delta\bar{L}(\epsilon, \delta) < 0 & \text{for every } \delta \text{ with } |\delta| \leq \epsilon^{\alpha+2} \text{ and } \frac{\delta}{|\delta|} \cdot \nu = -1. \end{cases}$$

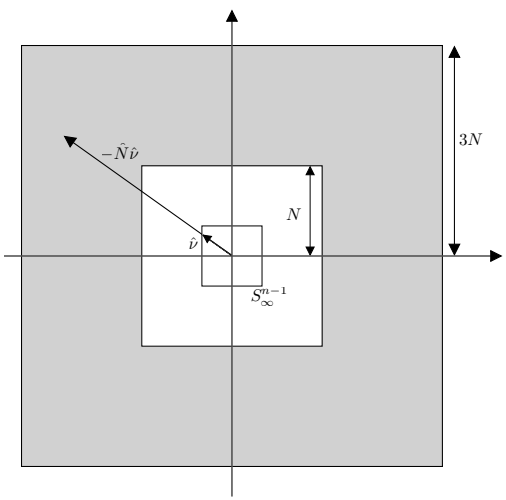

This statement shows that length-reducing procedures for triplets will not increase the discrete curvature indefinitely.

Discrete Birkhoff: fixed grid

Consequences from curvature bound

Proposition

Discrete Birkhoff algorithm leaves bounds on first and second difference quotients (curvature) invariant; it also preserves a graph structure.

Corollary

There exists an invariant neighbourhood (defined via N from the Proposition) of q_a and q_b such that suitable initial polygons cannot leave the neighbourhood under iteration.
The Birkhoff iteration for a fixed grid stops after finitely many steps, giving the approximation γ_1.

Refinement

Core arguments

Define

$$\epsilon_{k+1} := 2^k \epsilon_0 \text{ and } \delta_k := \left(\frac{2}{3}\right)^k \epsilon_k^2$$

Output of Birkhoff procedure at level k will be denoted γ_k.

Theorem

The sequence γ_k converges in $C^\beta([0,1]; S)$ for any $\beta \in (0,1)$ to a limit γ, and the limit curve γ solves the geodesic equation and hence is after time-reparametrisation a trajectory for the Hamiltonian boundary value problem.

Element of the proof:

- Argument so far relies crucially on discrete curvature bound.
- Potential problem: refinement $k \to k+1$ doubles discrete curvature.
- However, one application of Birkhoff at level $k+1$ reduces discrete curvature to the bound at step k (this follows from arguments giving existence of invariant region).

Summary: Convergence result

Scalings

- first scale: ϵ, second scale: $\delta = \epsilon^{2+\alpha}$ with $\alpha > 0$;
- the discretisation of the length functional necessarily has to be finer that the scaling δ in normal direction (e.g., ϵ^3).

Summary of results so far

1. Given q_a, q_b, by choosing E large enough we can show the existence of a trajectory connecting q_a and q_b and give a convergent numerical approximations.
2. Given E and q_a the same applies for suitable choices of q_b.

Remarks

- There are situations in which these three scales *cannot* be avoided (though they are of course not always required).
- In the Maupertuis formulation, one can also use Finite Elements to solve the nonlinear elliptic equation. This may be more efficient but uses higher derivatives (Christoffel symbols) of potential V.

Example: computational effort

Toy model

Consider $V(q) := exp(-\eta m \cdot q)$ with $\eta > 0$, $m, q \in \mathbb{R}^n$. Then (code in C, double precision, not parallel):

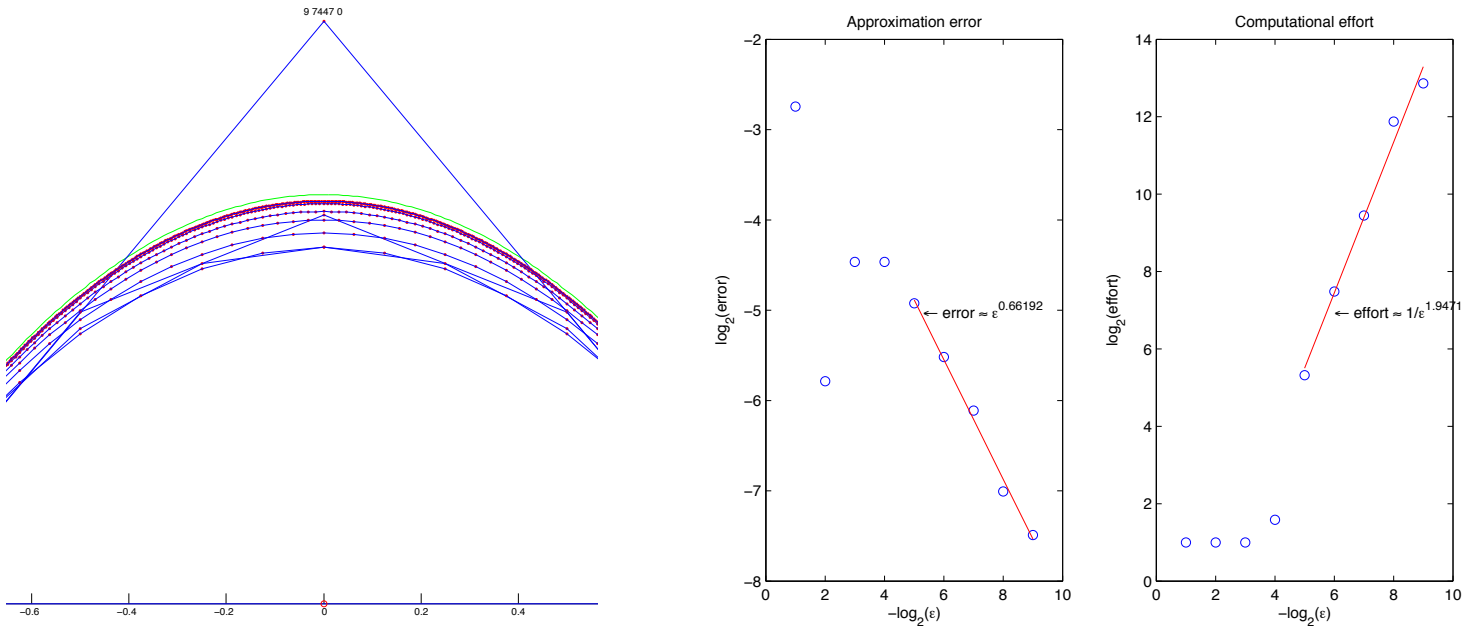

Figure: Exponential metric, $n = 2$, left: approximations (blue) and analytic solution (green). Right: Error approxmately $\sqrt{\epsilon}$, expenses approximately ϵ^{-2}

Advantage of approach: Parallelisation straightforward.

Example: computational effort

Toy model

The requirement that δ is small is not an artefact: gridlock occurs with δ too large.

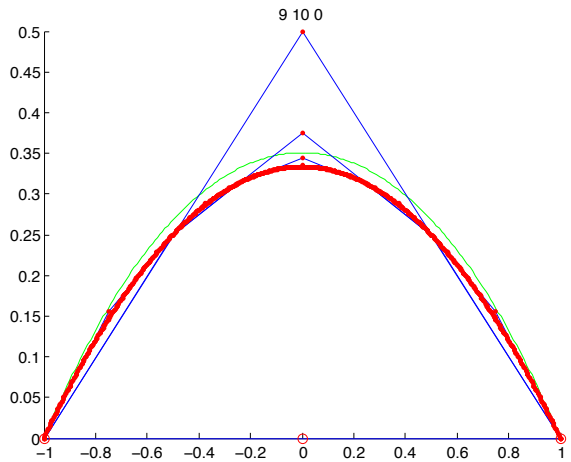

Figure: Gridlock for large stepsize δ

Natural approach: use more efficient method (e.g., flow method) first and then method described above.

A flow model algorithm for Jacobi's method

Sketch of algorithm

Schwetlick and Z., *J. Chem. Phys.*, **130** (2009), 124106: Use Jacobi formulation, but now implement a discrete flow inspired by Birkhoff.

Difficulty: metric is not Euclidean. Thus: approximate curve *and* metric, the latter by a piecewise constant one.

1. Input: a polygonal curve γ joining given configurations q_a and q_b inside the configuration manifold, $\gamma \subset Q$. We represent γ by its nodes $q(l)$, $l = 1, \ldots, L$, with $q_a = q(0), \ldots, q(L) = q_b$.
2. Approximate the metric g in a suitable neighbourhood of the curve by a piecewise Euclidean metric, such that the metric in the vicinity of a discretisation point $q(l)$ is given by the metric of that point, $g(q(l)) = E - V(q(l))$.

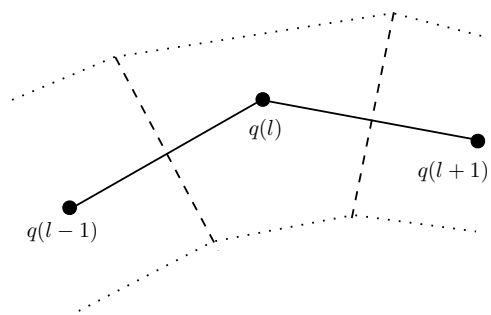

Figure: Sketch of the algorithm's Steps 1 and 2. In each region, the metric is Euclidean

A flow model algorithm for Jacobi's method

Sketch of algorithm

3. Iteratively single out three neighbouring discretisation points and move the middle one to decrease length.
4. Under iteration, neighbouring points can come close to each other faster than neighbouring points further away from the boundary $V(q) = E$. This normally leads to an increasingly uneven distribution of points during the iteration. We thus reparametrise the curve by arc-length to avoid a clustering of discretisation points.

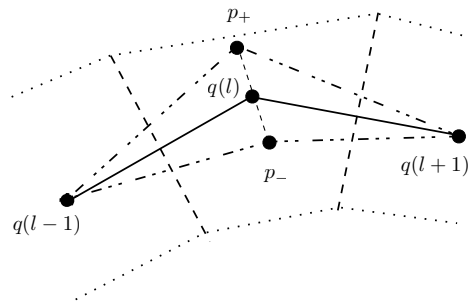

Figure: Sketch of the algorithm's Steps 3 and 4. The points $p_\pm$ are indicated; the vector ν^i defines the line joining p_+ and p_-. The curves joining $q(l-1)$, $p_\pm$ and $q(l+1)$ are shown as dashed-dotted lines.

Step 3 (Flow model)

Consider the flow of $q(l)$ in the direction of the normal ν^i. In continuous setting:

$$\frac{\partial}{\partial s} q(l) = -\nabla J\left(q(l)\right) \nu^i. \tag{5}$$

Mimic in discrete setting:

- Discretised tangent vectors: $\tau_- := q(l) - q(l-1)$ and $\tau_+ := q(l+1) - q(l)$. The mean $\tau := \frac{1}{2}\left(\tau_- + \tau_+\right)$ is then an averaged discrete tangent vector at $q(l)$.
- Let ν^i be a normalised unit vector orthogonal to τ.
- Approximate the gradient of the length functional as follows. For $\delta > 0$, we consider the points $p_\pm := q(l) \pm \delta\nu^i$.
- Let J_+ be the energy of the segment consisting of two lines joining $q(l-1)$ and $q(l+1)$ via p_+ (with respect to the piecewise Euclidean metric). Define J_- analogously.
- Then discrete gradient flow

$$q(l)^{\text{new}} := q(l) - \Delta\xi \cdot \left(J_+ - J_-\right) \nu^i. \tag{6}$$

Example: Collinear reaction

Example: Collinear reaction $\mathrm{H} + \mathrm{H}_2 = \mathrm{H}_2 + \mathrm{H}$

Simplest chemical reactions, common testing ground for computational studies of chemical reaction kinetics. Completely captured by two coordinates R_1 $(= R_{12})$ and R_2 $(= R_{23})$.
Potential energy: *ab initio* potential surface for linear H_3 (Liu, *J. Chem. Phys.*, **58** (1973), 1925–1937).

$$V(R_1, R_2) = V_0 + \sum_{j=1}^{2} V_{H_2}(R_j) + \exp(-\gamma(R_1 + R_2)) \times \sum_{k=0}^{n} \sum_{j=0}^{[k/2]} C_{k-j,j} \left(R_1^{k-j} R_2^j + R_1^j R_2^{k-j} \right), \quad (7)$$

with the potential energy $V_{H_2}(R_j) = -1 + \exp\left(-\alpha R_j \sum_{l=0}^{m} a_j R_j^l\right)$. Here $n = 14$, $m = 8$, $V_0 = 0.5$, $\alpha = 1.9140625$, and $\gamma = 1.5390625$.

Example: Collinear reaction

Simulations

Finite energy $E = -1.5\mathrm{au}$
(saddle-point energy is $E = -1.658\mathrm{au}$).
Reactant configuration and product near the entrance channel:

- Reactant configuration
  $R_1 = 3\mathrm{bohr}$, $R_2 = 1.4\mathrm{bohr}$
- Product configuration
  $R_1 = 1.4\mathrm{bohr}$, $R_2 = 3\mathrm{bohr}$

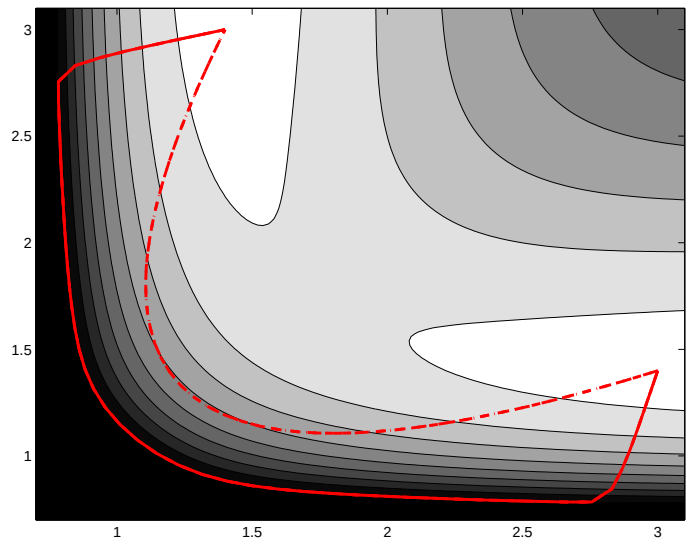

Figure: Initial curve (dashed) and its corresponding local minimum of the length functional (solid)

Example: Collinear reaction

Simulations

Same E as above, but different initial curves (lower dasher and upper dashed-dotted curves). Both converge to the inscribed curve (solid).

The 2D case is special: comparison principle holds, all curves initially inscribed by the two outer curves will converge to the same minimum.

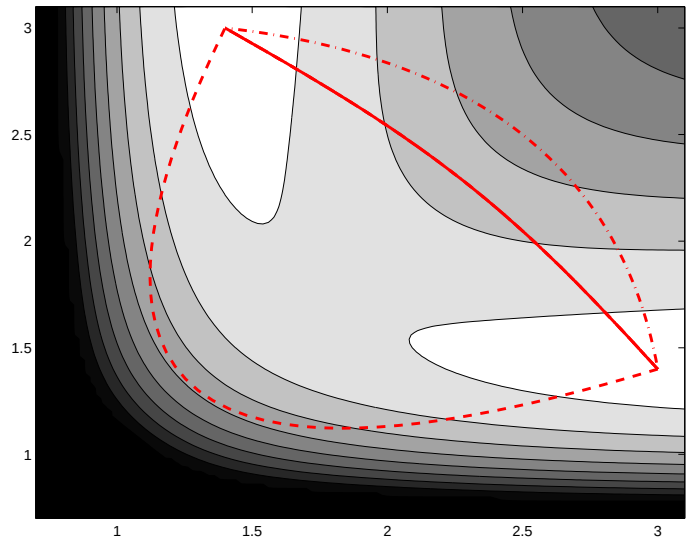

Figure: Two initial curves (lower dasher and upper dashed-dotted curves) and their corresponding local minimum (solid curve). The solid curve describes a trajectory joining the initial and final state

Example: Collinear reaction; saddle point approximation

Simulations

Again $E = -1.5\mathrm{au}$. The thin region between the two middle curves approximates the position of a saddle curve.

(Bisection procedure employed to find saddle connections: initial curves are deformed until they enter the regions already identified as domains of attraction of the local minima. Thus curves in the stable manifold of the saddle are approximated. An iteration of the procedure then approaches the saddle curve. Numerically not cheap.)

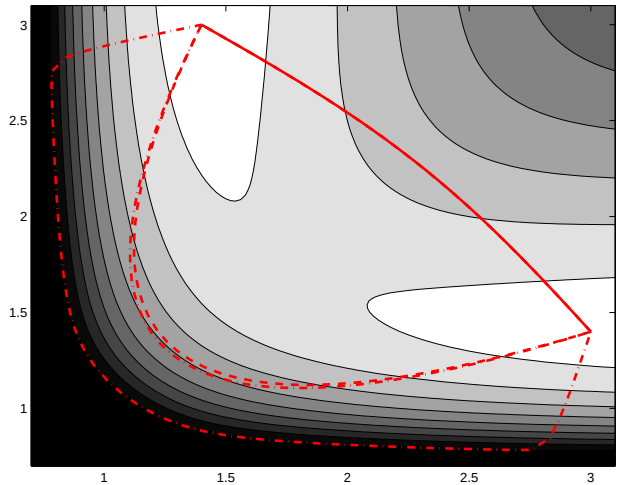

Figure: Separation of two domains of attraction: the upper dashed curve converges to one local minimum (solid curve), the nearby dash-dotted curve converges to different local minimum along the boundary (outer dash-dotted curve).